

Predetermination of potential plastic hinges on reinforced concrete frames using GFRP reinforcement

Dominik KUERES^{a*}, Dritan TOPUZI^b, Maria Anna POLAK^a

^a Department of Civil and Environmental Engineering, University of Waterloo, Waterloo, ON N2L 3G1, Canada

^b Schoeck Canada Inc., Ottawa, ON K1P 5G3, Canada

*Corresponding author. E-mail: dominik.kueres@hm.edu

© Higher Education Press 2022

ABSTRACT In the past, glass fiber-reinforced polymer (GFRP)-reinforcement has been successfully applied in reinforced concrete (RC) structures where corrosion resistance, electromagnetic neutrality, or cuttability were required. Previous investigations suggest that the application of GFRP in RC structures could be advantageous in areas with seismic activity due to their high deformability and strength. However, especially the low modulus of elasticity of GFRP limited its wide application as GFRP-reinforced members usually exhibit considerably larger deformations under service loads than comparable steel-reinforced elements. To overcome the aforementioned issues, the combination of steel and GFRP reinforcement in hybrid RC sections has been investigated in the past. Based on this idea, this paper presents a novel concept for the predetermination of potential plastic hinges in RC frames using GFRP reinforcement. To analyze the efficiency of the concept, nonlinear finite element simulations were performed. The results underscore the high efficiency of hybrid steel-GFRP RC sections for predetermining potential plastic hinges on RC frames. The results also indicate that the overall seismic behavior of RC structures could be improved by means of GFRP as both the column base shear force during the seismic activity as well as the plastic deformations after the earthquake were considerably less pronounced than in the steel-reinforced reference structure.

KEYWORDS glass fiber-reinforced polymer, GFRP, hybrid section, plastic hinge, seismic design, reinforced concrete

1 Introduction

The design and detailing of reinforced concrete (RC) structures is usually governed by dead and live loads at ultimate and serviceability limit states. In areas with seismic activity, severe loads caused by earthquakes may also occur. When subjected to high seismic loads, RC structures exhibit inelastic deformations leading to a redistribution of internal forces. As a result, some structural elements might be subjected to higher internal forces than considered in the original design. Consequently, these elements might fail during an earthquake if redistribution of internal forces is not sufficiently taken into account. Depending on the importance of the element with respect to the overall structural behavior, its failure might even trigger a progressive collapse of the whole structure (e.g., 2011 Christchurch Earthquake [1]).

Moment-resisting RC frame buildings are often constructed in areas with seismic activity where they are subject to severe loads and must comply with high displacement demands. When subjected to high seismic loads, inelastic deformations at particular locations of the structural system are intended to dissipate energy. This reduces the seismic effects on the structure. In RC frames, these inelastic deformations usually occur over a finite length (plastic hinge). Depending on the detailing of the structural elements, plastic hinges may occur either in columns or in beams. As the formation of plastic hinges in columns is detrimental to the stability of the structure, it is highly desirable that inelastic deformations concentrate in beams. Moreover, the energy dissipated in beam-sway systems is higher than in column-sway systems. Consequently, the design and detailing of RC frames in seismic areas should consider the formation of potential plastic hinges in beams.

In this paper, a new concept for the predetermination of

potential plastic hinges on RC frames is presented. The hybrid concept combines glass fiber-reinforced polymer (GFRP) reinforcement with conventional steel reinforcement at the desired plastic hinge location. GFRP reinforcement has a higher short-term strength and a lower modulus of elasticity compared to steel reinforcement [2]. Based on these material properties, it is assumed that the location of plastic hinges can be efficiently controlled by means of hybrid beam regions. To verify this assumption, nonlinear finite element simulations were carried out underlining the high potential of hybrid steel-GFRP-reinforced cross-sections for the predetermination of potential plastic hinges on RC frames. Additionally, the investigations indicate that the mechanical properties of GFRP could be advantageous during earthquakes as hybrid plastic hinges reduced the seismic effects on the sample structure compared to conventional steel-only hinges. Obviously, the ratio of steel and GFRP reinforcement of the hybrid cross-section has an impact on the deformation behavior at serviceability limit state, which needs to be considered in the structural design for gravity loads.

2 Predetermination of plastic hinges on reinforced concrete frames

2.1 General

Since the predetermination of potential plastic hinges in RC frames is a very complex task, a considerable amount of research has been performed in this field over the past

decades. A variety of different hinge detailing techniques have been developed and both theoretically and experimentally analyzed. The following section briefly summarizes the most common beam hinge detailing concepts for RC frames described in literature. Moreover, the proposed hybrid steel-GFRP hinge reinforcement detailing is presented in more depth.

2.2 Conventional steel-reinforced plastic hinge detailing

Various plastic hinge detailing techniques using conventional steel reinforcement have been proposed in the literature. Among them, traditional techniques like strong column-weak beam connections have been suggested, which are still the basis of various codes of practice. The original technique of strong columns and weak beams has the disadvantage of plastic hinges forming directly at the column face leading to a considerable stiffness and strength deterioration of the connection. To avoid the unfavorable formation of plastic hinges at the column-beam joint, it is necessary to move the plastic hinge away from the column face [3,4]. In this context, the relocation of the plastic hinge can, for example, be achieved by increasing the cross-section height of the beam at the column face (e.g., haunches [5], Fig. 1(a)) or by special detailing of the conventional reinforcement (e.g., cross-bars [6], Fig. 1(b)). As both methods cause considerable effort on a construction site, other, more sophisticated techniques have been developed to reduce both construction time and costs. For example, headed bars (e.g., Ref. [7], Fig. 1(c)) or prefabricated reinforcing bar details (e.g., Ref. [8]) have been found to be efficient in

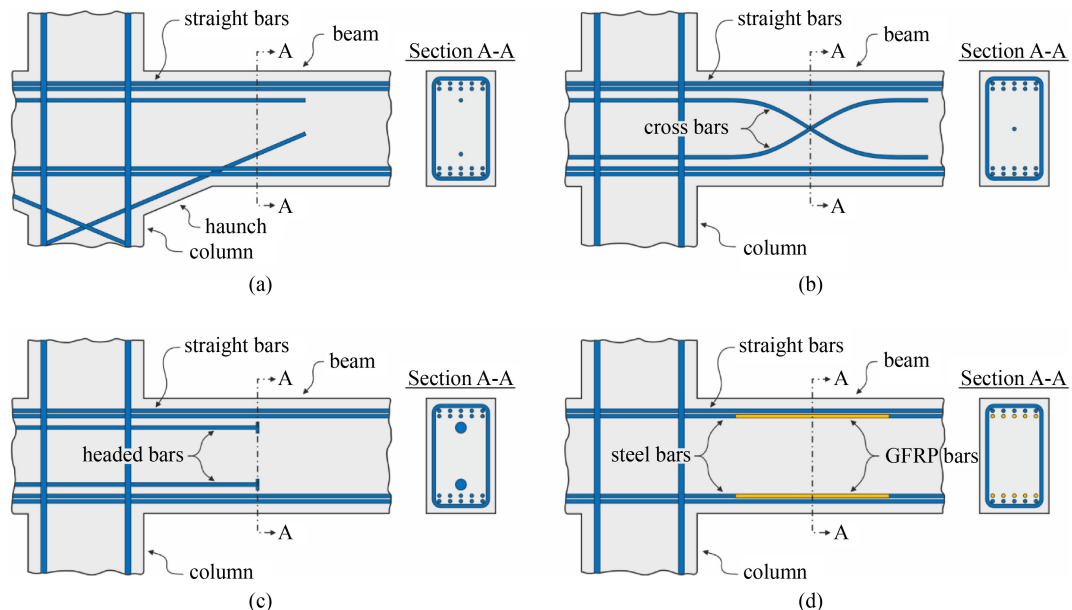


Fig. 1 Plastic hinge relocation concepts (transverse reinforcement not shown for the sake of clarity). (a) Relocated hinge detailing by use of haunches; (b) relocated hinge detailing by use of cross bars; (c) relocated hinge detailing by use of headed bars; (d) proposed relocated hinge detailing by use of hybrid steel-GFRP cross-sections.

relocating potential plastic hinges in beams. Nevertheless, despite the differences of the aforementioned plastic hinge detailing techniques in terms of cost efficiency and labor effort, their deformation capacity (i.e., energy dissipation during seismic activity) is comparable as it is mostly related to the yielding of the steel reinforcement.

2.3 Hybrid plastic hinge detailing using glass fiber-reinforced polymer reinforcement

GFRP has been commercially available as reinforcement for concrete structures for more than 20 years. Since the introduction to the market, GFRP reinforcement has been used usually as an alternative to steel reinforcement for durability reasons to avoid corrosion (e.g., bridge deck slabs). In addition, GFRP bars have been applied in situations where electromagnetic neutrality (e.g., magnetic resonance imaging equipment in hospitals) or high cuttability (e.g., temporary concrete structures at tunnel ends) are required [2]. In contrast to conventional steel bars, under tensile loading, GFRP bars exhibit a linear elastic behavior up to failure. While the short-term tensile strength of GFRP bars is usually significantly higher compared to steel bars, the modulus of elasticity is considerably lower. The differences of the mechanical properties lead to a different behavior under various loading scenarios, which have to be taken into account for ultimate and serviceability limit state design of GFRP-RC structures [9]. Besides the short-term properties, also the long-term properties of GFRP bars differ significantly from steel bars. In this context, influences of loading history, duration of loading, temperature and humidity strongly affect the mechanical properties of GFRP bars [2].

The behavior of GFRP-RC members under seismic loading has been investigated by several researchers (e.g., Refs. [10–15]). The test results suggest that the use of GFRP bars could be advantageous in regions with high seismic activity due to their high deformability and high strength. Taking into account the GFRP properties, the replacement of the entire longitudinal steel reinforcement with GFRP reinforcement at the desired plastic hinge location of a RC frame would result in a higher rotational capacity (ability of sustain high rotations without loss of strength) of the cross-section without adversely affecting its flexural strength. However, with respect to the overall behavior of the beam-column connection, the complete substitution of longitudinal steel reinforcement with GFRP reinforcement might also have a negative impact since the column demand would be higher. As a result, the desired predetermination of hinges in the beam rather than in the column (or near the column) becomes considerably more difficult, which is also indicated by the test results presented in Ref. [14]. Another issue related to GFRP-only connections is associated with the lower

modulus of elasticity as the deformations of the GFRP-RC beam would be considerably larger compared to the conventionally reinforced beam resulting in cracking even under service loads. Nevertheless, as the higher rotational capacity of GFRP would only be needed in case of severe seismic activity, it can be postulated that a combination of steel and GFRP reinforcement could be efficiently applied in potential plastic hinges on RC frames to control the location of the hinge and to increase the energy dissipation during an earthquake. As a consequence, in this paper the effect of hybrid steel-GFRP hinges is investigated in more detail.

An example for a hybrid steel-GFRP hinge reinforcement detailing is schematically illustrated in Fig. 1(d). In accordance with the design of conventional steel-reinforced plastic hinges, the steel reinforcement at the hinge region should be designed to yield only when the structure is subjected to considerable seismic loads and remain elastic under serviceability gravity loads. As a result, under service loads, the GFRP reinforcement would have a minor effect on both the sectional strength (strain compatibility) and the structural response, which is also indicated by the existing investigations on flexural behavior of hybrid steel-GFRP beams (e.g., Refs. [16–19]). When subjected to severe seismic loads, the steel reinforcement would yield. At this point, any additional stress would be carried by the GFRP reinforcement allowing for an enhanced seismic response of the cross-section compared to the steel-only section. Another advantage of the proposed hybrid hinge detailing is the fact that any adverse influences of long-term loading do not occur as the GFRP bars would only be highly stressed over the short-time period of the earthquake.

3 Numerical investigations

3.1 General

In order to investigate the efficiency of the proposed hybrid steel-GFRP plastic hinge reinforcement detailing, nonlinear finite element simulations of a sample RC frame subjected to a recorded ground acceleration were performed. The simulations were conducted using the open source finite element platform OpenSees (Open System for Earthquake Engineering Simulations [20]). For the sake of comparison, various hinge reinforcement details were considered. In this context, hybrid hinge cross-sections with different ratios of steel and GFRP reinforcement were analyzed and the results were compared to a conventional steel-only solution. Moreover, the influence of the plastic hinge length and the magnitude of live loads on the efficiency of the proposed hybrid hinge detailing was investigated. The following sections summarize the basics of the numerical simulations and the results.

3.2 Sample reinforced concrete frame

The sample RC frame considered in the finite element simulations is depicted in Fig. 2(a). The three-story two-bay frame had a span length of 7000 mm and a story height of 3500 mm. The span length perpendicular to the center frame was 7000 mm. Besides the self-weight g ($\gamma_{RC} = 24 \text{ kN/m}^3$) of the frame and the adjacent slabs (depth $h_{slab} = 200 \text{ mm}$), a further dead load $\Delta g = 1.0 \text{ kN/m}^2$ was considered for the structural design. Also, a live load $q = 4.8 \text{ kN/m}^2$ (assembly areas) was assumed and the flexural design of the beams was performed neglecting any effects caused by moment redistributions between hogging and sagging moments. The concrete compressive strength was assumed as $f_c = 35 \text{ N/mm}^2$ and the yield strength of the steel reinforcement was taken as $f_y =$

400 N/mm^2 . The resulting cross-sections of the structural elements of the RC frame (designed without partial safety factors) are shown in Fig. 2(a). In this context, the beam cross-section had a width of 300 mm and a height of 500 mm. The longitudinal reinforcement of the beam cross-section for the hinge region (hogging moment) consisted of 10-15M steel bars ($E_s = 200000 \text{ N/mm}^2$, $f_y = 400 \text{ N/mm}^2$, $\phi_{nominal} = 16.0 \text{ mm}$ [21]) in both the tension and the compression zone. In the positive moment region (sagging moment), the longitudinal reinforcement was reduced to 5-15M steel bars ($E_s = 200000 \text{ N/mm}^2$, $f_y = 400 \text{ N/mm}^2$, $\phi_{nominal} = 16.0 \text{ mm}$ [21]) on each side of the cross-section. The column cross-section had dimensions of $500 \text{ mm} \times 500 \text{ mm}$ and was symmetrically reinforced by means of 20-25M steel bars ($E_s = 200000 \text{ N/mm}^2$, $f_y = 400 \text{ N/mm}^2$, $\phi_{nominal} = 25.2 \text{ mm}$ [21]). The sample frame

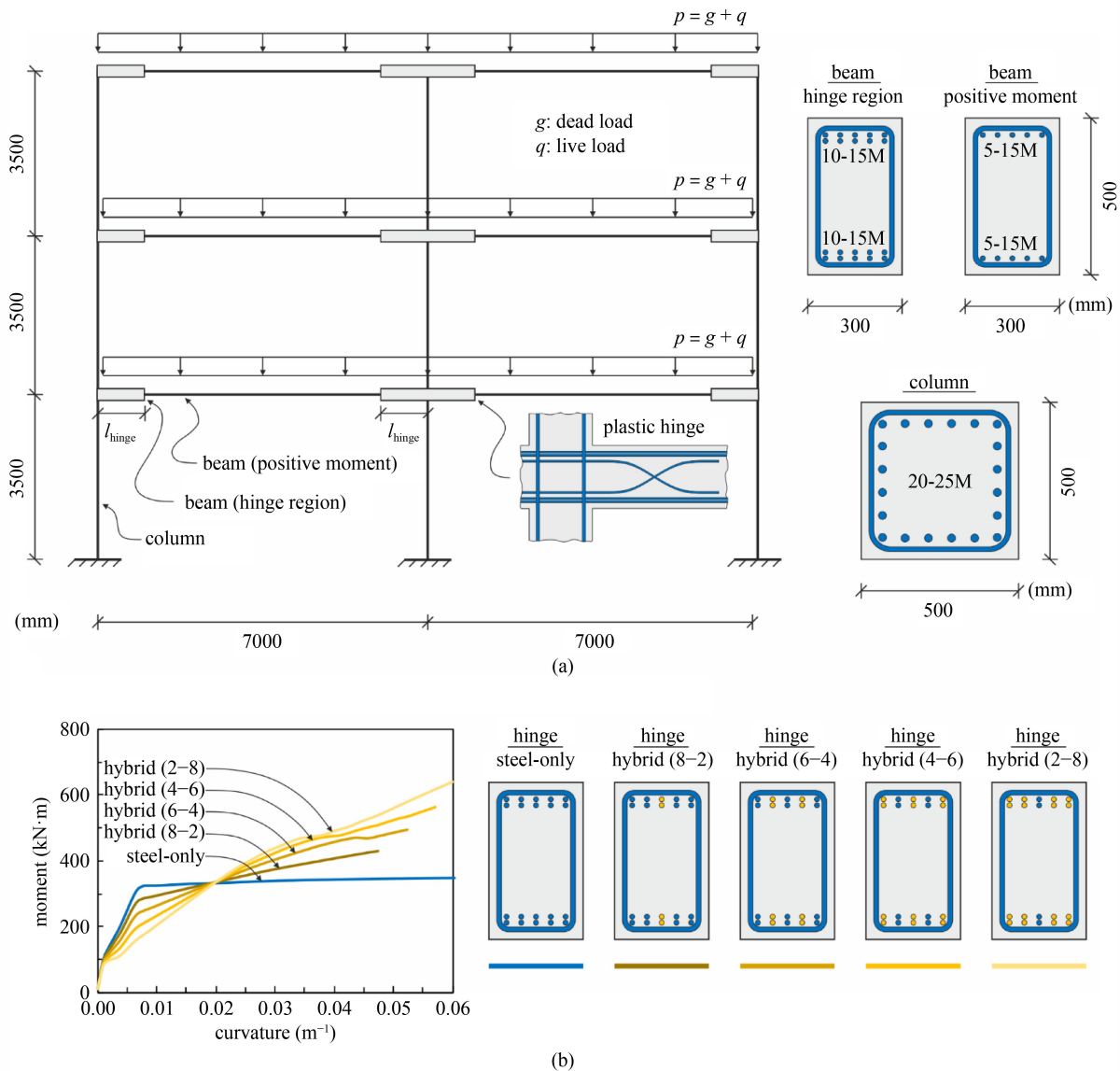


Fig. 2 Sample RC frame for nonlinear finite element simulations. (a) Structural system and cross-sections; (b) moment-curvature-relationships of investigated hinge cross-sections.

used in all the studies was not optimized for earthquake designs at this point. Nevertheless, the rather simple frame was chosen to study the comparative behavior (namely, steel only versus different types of hybrid reinforcement) of the proposed detail.

The moment-curvature-relationship of the steel-reinforced hinge cross-section is illustrated in Fig. 2(b) (blue curve) and can be divided into four branches. While the first branch is characterized by a stiff initial response, which is mostly related to the stiffness of the uncracked concrete, the second branch exhibits a reduced stiffness of the composite section as a result of cracking. At a certain deformation, no new cracks form and the contribution of concrete to the moment-curvature-response vanishes. As a result, the response in the third branch is governed by the contribution of the steel reinforcement until the yield strength is reached. After this point (fourth branch), the moment-curvature-relationship is dominated by yielding of the reinforcement and slight increases in moment capacity are associated with very large deformations (strain hardening of the steel reinforcement).

Besides the conventional steel-only cross-section, four additional hybrid steel-GFRP sections with different ratios of steel and GFRP reinforcement were considered in the hinge region to investigate the effect of hybrid hinges on the seismic behavior of RC frames in a systematic manner. In this context, 20% (Hybrid (8-2)), 40% (Hybrid (6-4)), 60% (Hybrid (4-6)), and 80% (Hybrid (2-8)) of the steel reinforcement of the original cross-section were substituted by GFRP reinforcement ($E_f = 60000 \text{ N/mm}^2$, $f_{fu} = 1000 \text{ N/mm}^2$, $\phi_{\text{nominal}} = 16.0 \text{ mm}$). The moment-curvature-relationships of the hybrid hinge sections are also depicted in Fig. 2(b). While the first branch of the curves of the hybrid sections is similar to the steel-only solution, the stiffness in the second and third branch is considerably lower. This observation is more pronounced as more steel reinforcement is substituted by GFRP reinforcement. Moreover, due to the reduced amount of steel reinforcement in combination with the smaller modulus of elasticity of the GFRP, yielding of the steel reinforcement starts at lower moment capacities. Nevertheless, compared to the moment-curvature-relationship of the steel-reinforced section in the fourth branch, the response of the hybrid sections is significantly steeper leading to considerable higher ultimate moment capacities.

3.3 Numerical model

The numerical simulations presented in this paper were performed by means of the finite element software OpenSees (Open System for Earthquake Engineering Simulations [20]). OpenSees is an object-oriented open source finite element platform developed at the University of California at Berkeley, USA, which can be used

for nonlinear simulations in earthquake engineering. As a benefit of the open source framework, many researchers have contributed to the development of the software by adding various components like element formulations, material models, solvers, etc. to the platform. Due to the TCL code-based structure, OpenSees can be efficiently applied to perform sophisticated numerical simulations of the response of structures under seismic actions.

Using the OpenSees environment, the columns and beams (hogging and sagging moment cross-sections) of the RC frame depicted in Fig. 2, were modeled by means of displacement-based beam-column elements with linear geometric transformation and five Gauss-Legendre integration points along the element length. In the simulations, the Newton-Raphson algorithm was applied and the cross-sections of both the column and beam elements were formulated based on a fibered section model assuming rigid bond between concrete and reinforcement (Fig. 3(a), Refs. [20,22]). The concrete behavior was modeled by means of the Concrete02 constitutive model available in OpenSees assuming linear tension softening (Fig. 3(b), Refs. [20,23]). In this context, the concrete properties of the section fibers confined by stirrups were calculated based on the modified Kent-Park procedure [24,25]. For the steel reinforcement, the Steel02 constitutive material law with isotropic strain hardening included in OpenSees was applied (Fig. 3(c), Refs. [20,26]) and the GFRP reinforcement was modeled linear-elastically until rupture (Fig. 3(d)). The material properties assumed for the numerical simulations are summarized in Table 1.

3.4 Discussion of results

3.4.1 General

The behavior of the sample RC frame depicted in Fig. 2(a) was simulated under both gravity loads and a combination of gravity and seismic loads. To investigate the differences between steel-only and hybrid steel-GFRP hinge reinforcement details, a total of five cross-sections with different ratios of steel and GFRP reinforcement were investigated (Fig. 2(b)). The results of the numerical simulations are presented and discussed in the following sections. Moreover, topics for future research are suggested.

3.4.2 Behavior under gravity loads

The behavior of the sample RC frame under gravity loads can be analyzed based on the numerical results shown in Fig. 4. For the simulations, the unfactored self-weight of the frame and the adjacent slabs (depth $h_{\text{slab}} = 200 \text{ mm}$) as well as an additional dead load of $\Delta g = 1 \text{ kN/m}^2$ were considered. Moreover, an unfactored live load of $q =$

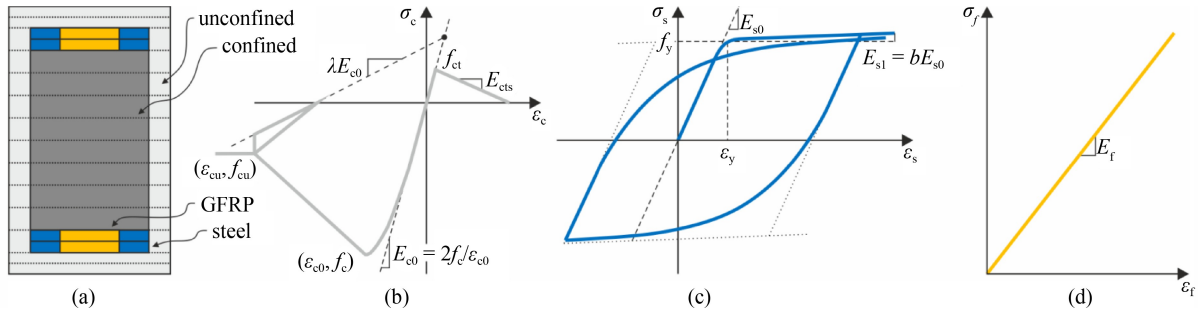


Fig. 3 Numerical formulation of cross-sections and materials. (a) Fibered hybrid steel-GFRP beam cross-section; (b) concrete constitutive model; (c) steel constitutive model; (d) GFRP constitutive model.

Table 1 Material properties for the numerical simulations

parameters	material		
	concrete	steel	GFRP
f_c (N/mm ²)	-35	—	—
ε_{c0}	-0.002	—	—
f_{cu} (N/mm ²)	-7	—	—
ε_{cu}	-0.004	—	—
λ	0.1	—	—
f_{ct} (N/mm ²)	3.2	—	—
E_{cts} (N/mm ²)	3210	—	—
f_y (N/mm ²)	—	400	—
E_s (N/mm ²)	—	200000	—
b	—	0.01	—
R_0	—	15	—
CR_1	—	0.925	—
CR_2	—	0.15	—
f_{fu} (N/mm ²)	—	—	1000
E_f (N/mm ²)	—	—	60000

Notes: f_c : concrete compressive strength; ε_{c0} : strain at maximum concrete compressive strength; f_{cu} : concrete crushing strength; ε_{cu} : strain at concrete crushing strength; λ : ratio between unloading slope at ε_{cu} and initial slope; f_{ct} : concrete tensile strength; E_{cts} : tension softening stiffness of concrete; f_y : yield strength of steel reinforcement; ε_y : yield strain of steel reinforcement; E_s : initial modulus of elasticity of steel reinforcement; b : strain-hardening ratio of steel reinforcement; R_0, CR_1, CR_2 : parameters to control the transition from elastic to plastic branches of steel reinforcement; f_{fu} : ultimate tensile strength of GFRP; E_f : modulus of elasticity of GFRP reinforcement.

4.8 kN/m² was applied to the structure. The hinge length was assumed as $l_{hinge} = 1000$ mm corresponding to the distance between the column face and the point of moment-contraflexure neglecting redistributions of inner forces. Moreover, the uniaxial constitutive material models were defined in accordance with Subsection 3.3.

Figure 4(a) depicts the stress in the longitudinal steel reinforcement in the tension zone of the beam at the center column in the second floor of the considered RC frame. In case of the conventional steel-reinforced cross-section, the tensile stress in the flexural reinforcement reaches a value of $f_{s,top} = 270$ N/mm². The difference between the computed stress and the yield strength

considered in the original design can be explained by redistributions between hogging and sagging moments due to cracking, which results in a smaller utilization of the hogging moment reinforcement. As a result of the substitution of steel with GFRP reinforcement, the tensile stresses in the steel reinforcement of the hybrid cross-sections are higher than in the steel-only section and increase with increasing amount of GFRP. However, for the investigated cross-sections, the hybrid hinge solution where 80% of the steel reinforcement is replaced with GFRP reinforcement (Hybrid (2-8)) is the only section exhibiting yielding of the steel reinforcement.

The stresses in the top GFRP reinforcement $f_{f,top}$ at the center column (second floor) of the RC frame are shown in Fig. 4(b). Depending on the section, the computed stresses vary between approximately 9% and 18% of the ultimate tensile strength of GFRP bars ($f_{fu} = 1000$ N/mm²). The low stresses in the GFRP reinforcement can be explained by the low modulus of elasticity of GFRP supporting the assumption that GFRP has a minor impact of the response of hybrid steel-GFRP cross-sections under gravity loads, especially if the steel reinforcement does not reach the yield strength. This observation is also emphasized by the computed mid-span deflections of the beam in the second floor of the sample RC frame (Fig. 4(c)). While the steel-only solution exhibits a deflection of $w = 9.9$ mm, the deflection of the hybrid section with 40% GFRP reinforcement (Hybrid (6-4)) is only approximately 20% larger. If more steel is substituted with GFRP, the mid-span deflection increases. Nevertheless, all investigated cross-sections fulfill the maximum permissible deflection criterion ($l_{span}/360$) defined in Ref. [27] for steel-RC structures.

The analysis of the sample RC frame under gravity loads underscore the potential of hybrid steel-GFRP-reinforced cross-sections compared to exclusively GFRP-reinforced sections. In this context, the investigations suggest that a combination of steel and GFRP reinforcement at certain locations of the structural system does not imply severe deformations under gravity loads. Also, due to the low modulus of elasticity, the stress in the GFRP reinforcement is very low in hybrid sections reducing adverse effects of long-term loading on the tensile strength of GFRP bars. Obviously, both the

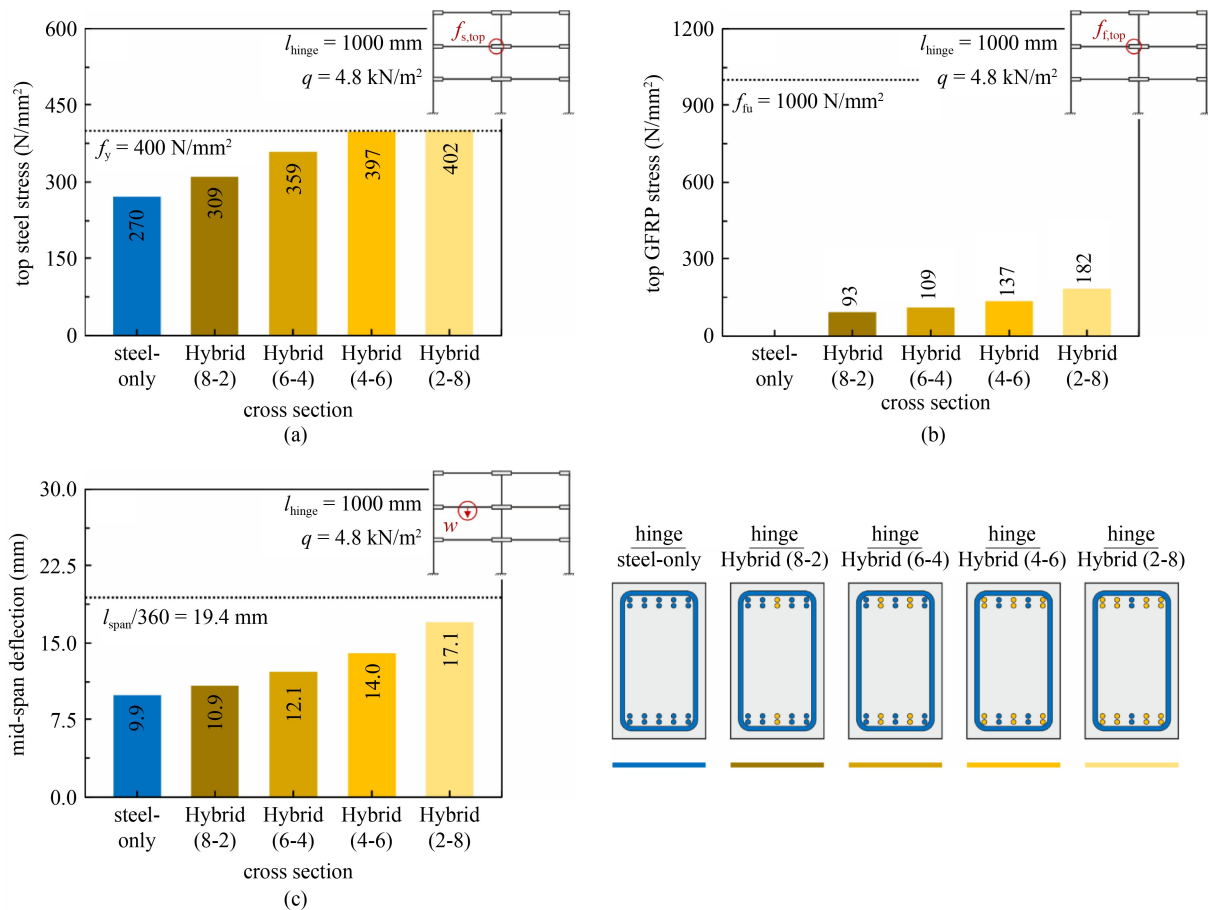


Fig. 4 Behavior of the sample RC frame under gravity loads. (a) Tensile stress in longitudinal steel reinforcement at the center column (second floor); (b) tensile stress in longitudinal GFRP reinforcement at the center column (second floor); (c) deflection at mid-span of the beam in the second floor.

deformation behavior and the utilization of the GFRP reinforcement are strongly affected by the ratio of steel and GFRP, which need to be considered in the design of hybrid RC structures.

3.4.3 Behavior under seismic loads

To investigate the behavior of the sample RC frame (Fig. 2(a), fundamental periods: $T_1 = 0.89 \text{ s}$, $T_2 = 0.24 \text{ s}$, and $T_3 = 0.11 \text{ s}$) under seismic actions, nonlinear time-history analyses of the frame subjected to the recorded 1940 El Centro Earthquake ground acceleration (north-south component) were conducted. Besides the conventional steel-only solution, four additional hybrid steel-GFRP-reinforced cross-sections (Fig. 2(b)) were considered in the hinge region. For the simulations, the same dead loads for the gravity load case (Subsubsection 3.4.2) were assumed. The unfactored live load was taken as $q = 0.5 \times 4.8 = 2.4 \text{ kN/m}^2$ and the hinge length was set to $l_{\text{hinge}} = 1000 \text{ mm}$. Moreover, the uniaxial constitutive material models were defined as described in Subsection 3.3. Some of the main results of the numerical simulations are presented in Figs. 5–7.

Figure 5(a) depicts the steel strain $\varepsilon_{s,\text{top}}$ in the top flexural reinforcement of the steel-reinforced hinge region located at the second floor of the center column of the sample frame as a function of the time of the imposed ground acceleration (solid blue line). At the beginning of the time-history analysis, the top steel strain is clearly below the yield strain (dotted black line). Nevertheless, after a short time period, the flexural reinforcement at the top face of the steel-reinforced cross-section reaches the yield strain as a result of the imposed ground acceleration indicating a plastic hinge forming at the desired location. With increasing time, the strain in the steel reinforcement increases far beyond the yield strain leading to considerable plastic deformations at the end of the seismic activity. Similar to the behavior of the sample frame under gravity loads, the initial strains in the top steel reinforcement $\varepsilon_{s,\text{top}}$ of the hybrid cross-sections (solid yellow lines) are larger compared to the steel-only solution (Figs. 5(b)–5(d)). As a consequence, plastic hinges form at an earlier stage of the imposed ground acceleration indicating the effect of the proposed combination of steel and GFRP reinforcement for the predetermination of potential plastic hinges on RC frames. With increasing time however, the strains in the

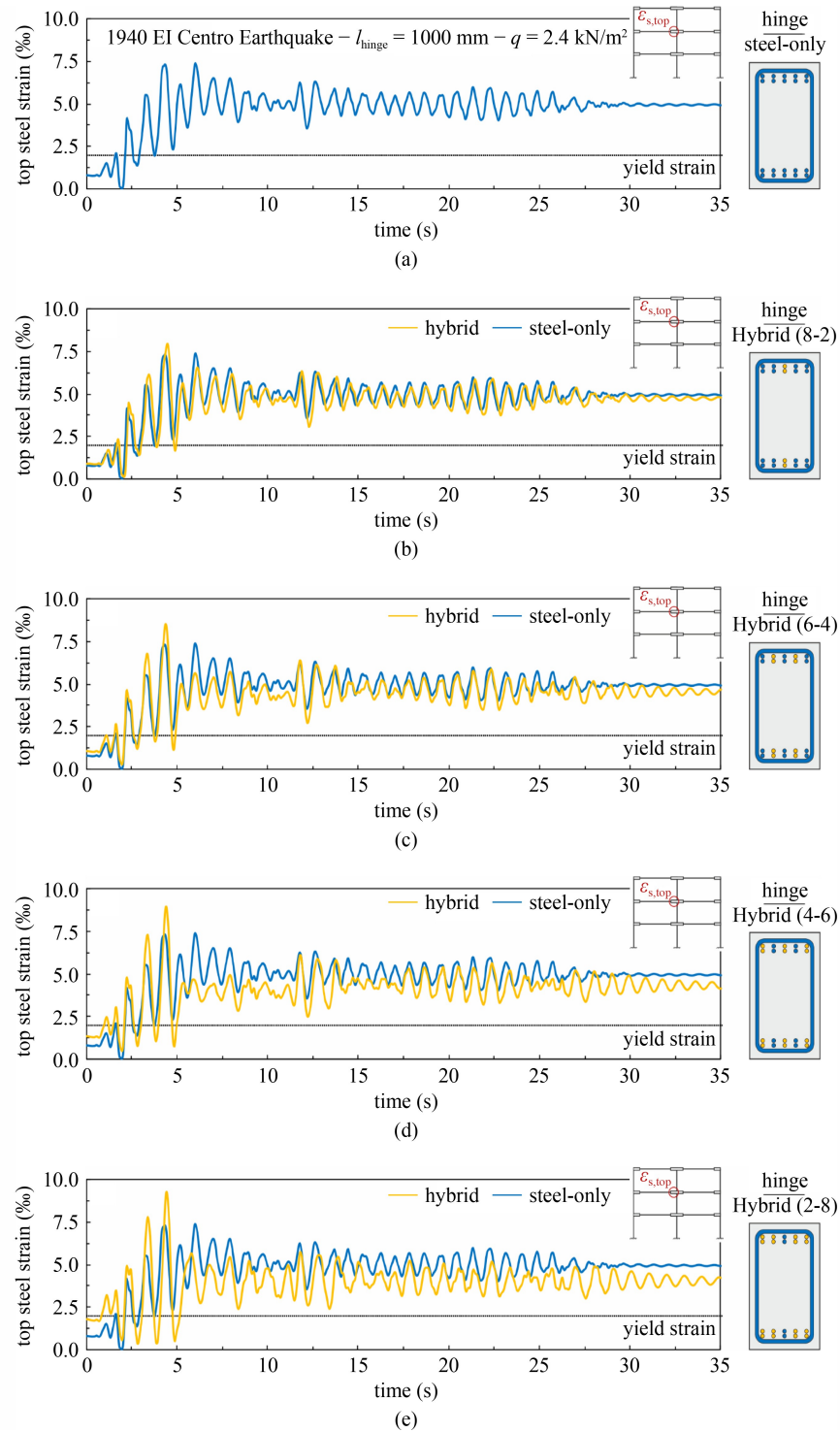


Fig. 5 Top steel reinforcement strain at the center column (second floor) of the sample RC frame. (a) Steel-only hinge; (b) Hybrid (8-2) hinge; (c) Hybrid (6-4) hinge; (d) Hybrid (4-6) hinge; (e) Hybrid (2-8) hinge.

top steel reinforcement of the hybrid sections, i.e., plastic deformations, are lower compared to the steel-only hinge. This observation can be explained by the linear-elastic behavior of the GFRP bars in combination with their high tensile strength. Therefore, the GFRP bars force the hybrid sections back towards their initial state. Obviously, this effect is more pronounced for hybrid sections

with high amounts of GFRP reinforcement.

The corresponding bottom concrete strain $\epsilon_{c,bot}$ measured on the opposite face of the investigated beams in the hinge region is illustrated in Fig. 6 as a function of the time of the imposed ground acceleration. In case of the conventional steel-only hinge reinforcement detailing (Fig. 6(a)), the concrete strain clearly remains below the

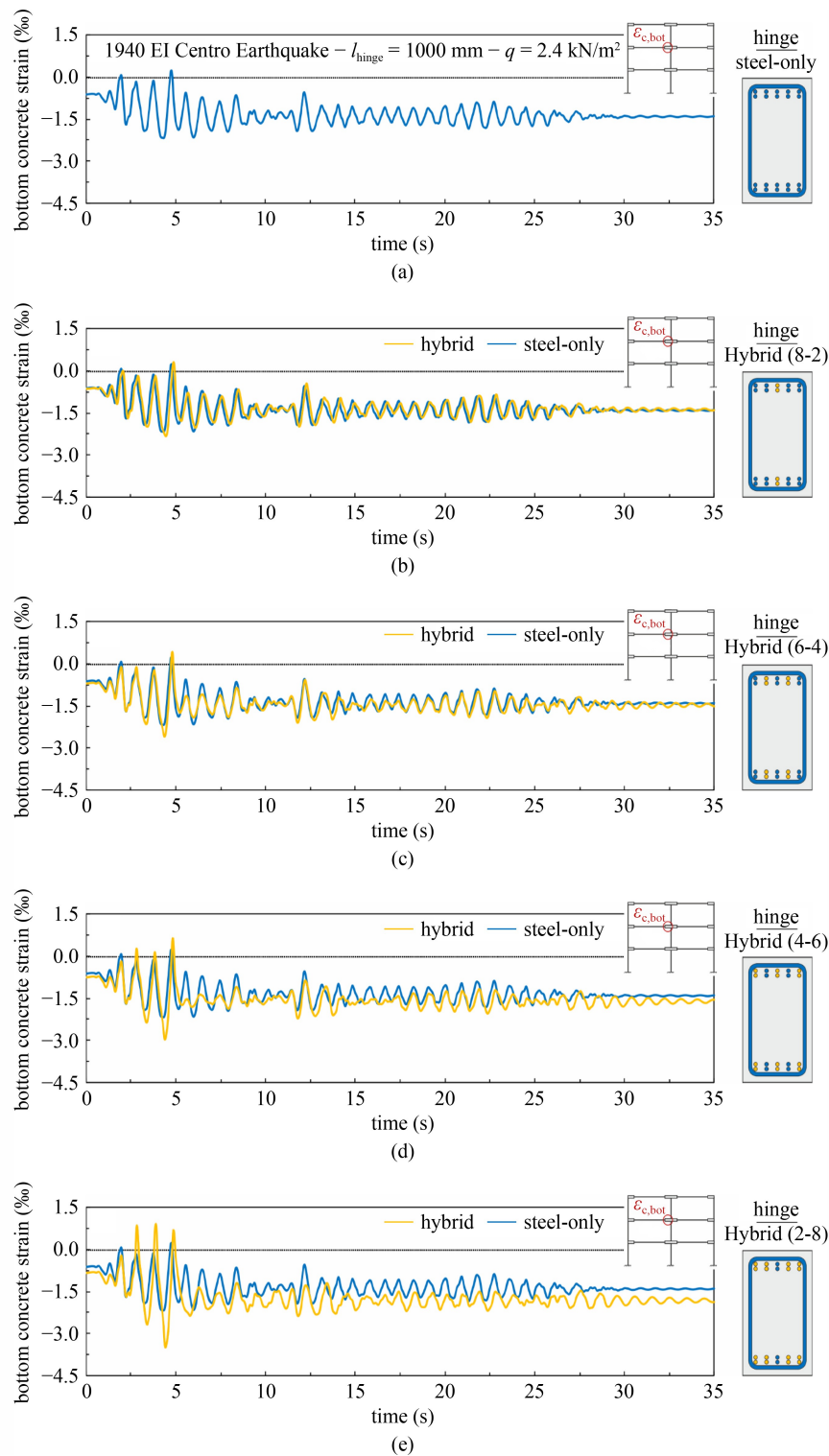


Fig. 6 Bottom concrete strain at the center column (second floor) of the sample RC frame. (a) Steel-only hinge; (b) Hybrid (8-2) hinge; (c) Hybrid (6-4) hinge; (d) Hybrid (4-6) hinge; (e) Hybrid (2-8) hinge.

crushing strain of concrete (Table 1). The hybrid hinge sections with low amounts of GFRP reinforcement show similar bottom concrete strains over the duration of the earthquake (Figs. 6(b) and 6(c)). In contrast, for the hybrid sections with higher amounts of GFRP

reinforcement, the computed compressive strains $\varepsilon_{c,bot}$ are larger compared to the steel-only solution (Figs. 6(d) and 6(e)). Nevertheless, the concrete crushing strength is not reached in any of the performed simulations.

As a consequence of the structural deformations caused

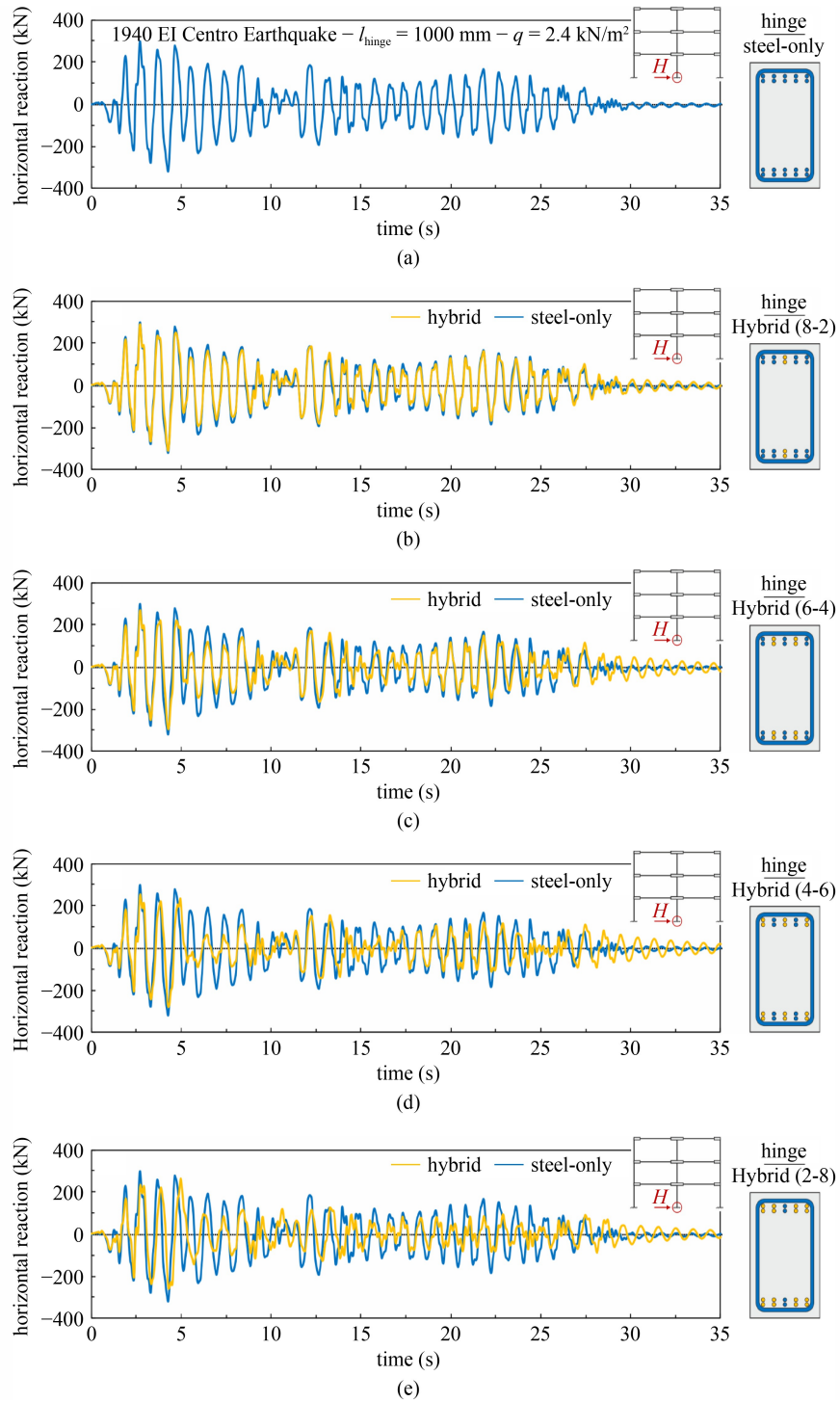


Fig. 7 Horizontal reaction at the center column of the sample RC frame. (a) Steel-only hinge; (b) Hybrid (8-2) hinge; (c) Hybrid (6-4) hinge; (d) Hybrid (4-6) hinge; (e) Hybrid (2-8) hinge.

by the ground acceleration, shear forces are introduced in the columns of the sample structure. Figure 7 depicts the recorded horizontal reaction forces H at the center column of the investigated steel-reinforced and steel-GFRP-RC frames. The horizontal reaction force at the center column is zero at the beginning of the time-history analysis for all investigated cases. Then, the computed

absolute values of the reaction forces first increase and later decrease oscillating around zero as the seismic activity continues. In this context, the recordings show peak reactions of more than 300 kN for the reference frame (Fig. 7(a)). The comparison with the hybrid RC frames (Figs. 7(b)–7(e)) reveals reduced peak reaction forces depending on the ratio of steel and GFRP

reinforcement. The highest reduction in peak reaction force is approximately 20% for the section with 80% GFRP reinforcement (Hybrid (2-8), Fig. 7(e)). Besides the reduction in peak reaction force, it is also interesting to note that the GFRP reinforcement seems to have an overall positive influence on the damping behavior of the structure as the seismic effects are less pronounced for the investigated hybrid RC frames than for the reference frame.

3.4.4 Parametric studies

To further analyze the seismic behavior of the sample RC frame with different plastic hinge details, additional nonlinear time-history analyses of the frame were

conducted. In this context, the effect of the length of the plastic hinge region as well as the magnitude of the live load were investigated. The hinge length was varied between $l_{\text{hinge}} = 500$ and 1500 mm (for $q = 2.4 \text{ kN/m}^2 = \text{constant}$) and the live load was assumed between $q = 0.0$ and 4.8 kN/m^2 (for $l_{\text{hinge}} = 1000 \text{ mm} = \text{constant}$). Figures 8 and 9 illustrate some of the main results of the parametric studies.

Figure 8(a) depicts the strain in the top flexural reinforcement of the steel-reinforced plastic beam region at the center column (second floor) over the time of the analysis. The results indicate that the length of the plastic hinge region has a significant influence on the computed strains in the flexural reinforcement. In this context, the strains in the top steel reinforcement increase

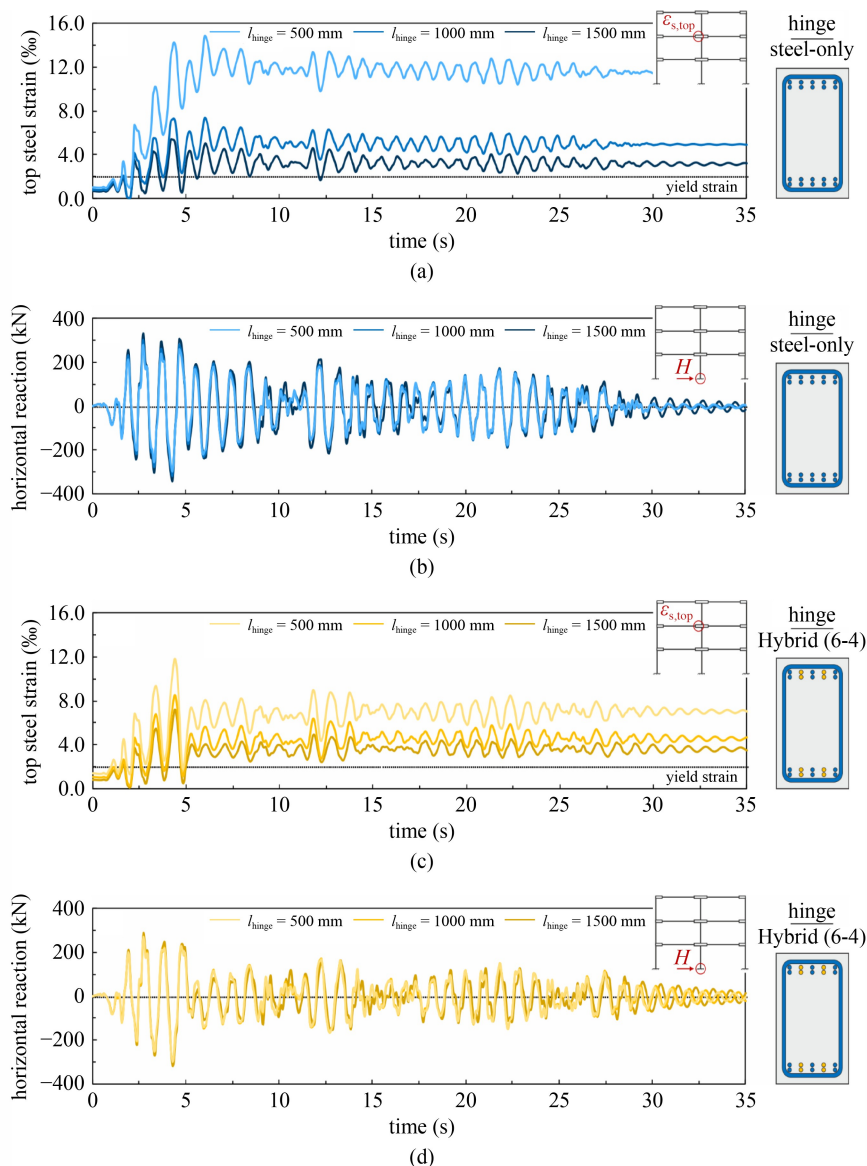


Fig. 8 Parametric study on the influence of the plastic hinge length on the seismic behavior of the sample RC frame. (a) Top steel strain at the center column (second floor) for the steel-only hinge; (b) horizontal reaction at the center column for the steel-only hinge; (c) top steel strain at the center column (second floor) for the Hybrid (6-4) hinge; (d) horizontal reaction at the center column for the Hybrid (6-4) hinge.

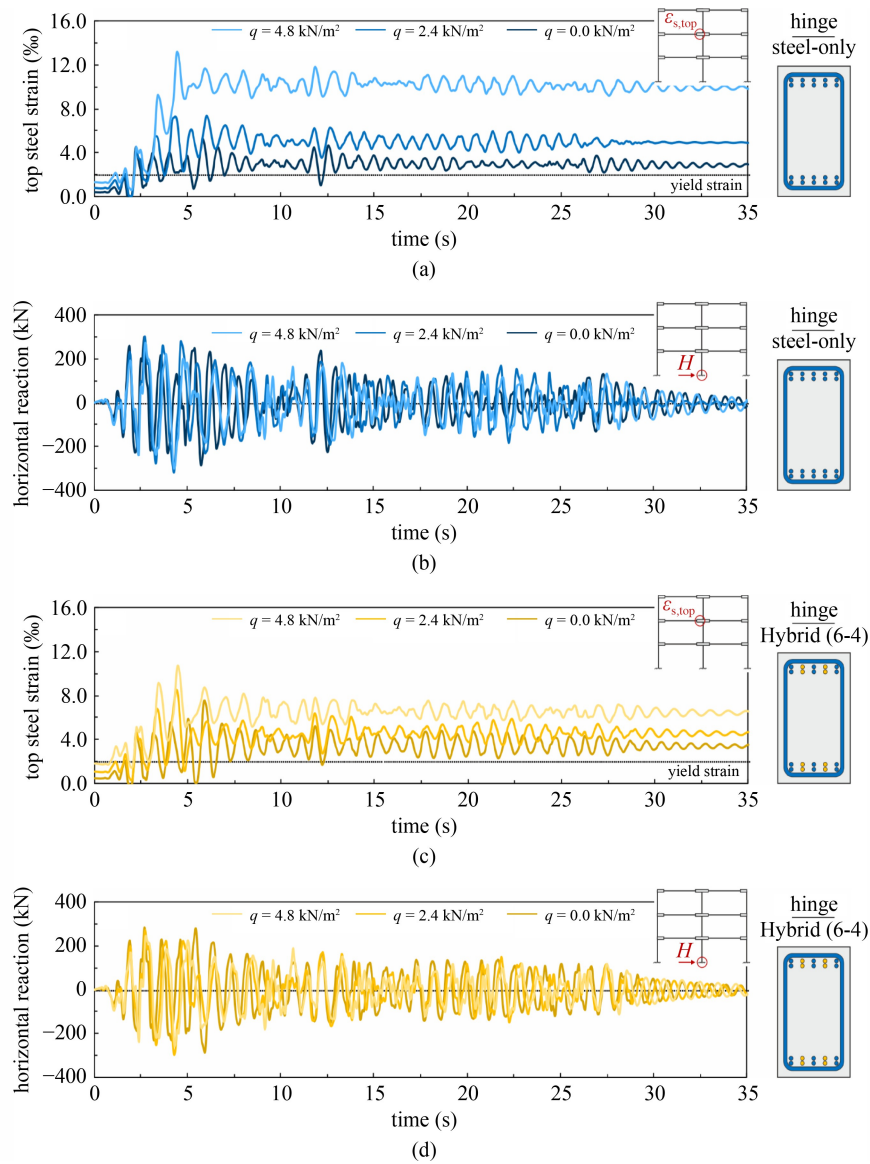


Fig. 9 Parametric study on the influence of the magnitude of the live load on the seismic behavior of the sample RC frame. (a) Top steel strain at the center column (second floor) for the steel-only hinge; (b) horizontal reaction at the center column for the steel-only hinge; (c) top steel strain at the center column (second floor) for the Hybrid (6-4) hinge; (d) horizontal reaction at the center column for the Hybrid (6-4) hinge.

significantly with decreasing hinge length resulting in very large plastic deformations of the cross-section (e.g., $l_{\text{hinge}} = 500 \text{ mm}$, Fig. 8(a)). The differences between the investigated cases can be explained by the fact that less redistributions between hogging and sagging moments may occur as a result of the reduced hinge length. Nevertheless, due to the larger deformations of the hinge cross-section with decreasing hinge length, more energy is dissipated during the earthquake leading to slightly lower horizontal reactions at the center column (Fig. 8(b)). Similar observations can be made for the hybrid RC frames. However, the effect is significantly less pronounced for hybrid frames (e.g., Hybrid (6-4) beam, Figs. 8(c) and 8(d)) since less redistributions between hogging and sagging moment may occur.

The parametric study on the influence of the magnitude of the live load on the seismic response of the sample RC frame reveals similar tendencies as the study on the hinge length. In this context, the strain in the top reinforcement of the steel-reinforced hinge section increases with increasing live load resulting in the formation of plastic hinges at an earlier stage of the earthquake (Fig. 9(a)). Moreover, the applied load of the investigated frames differ due to the different magnitudes of live loads resulting in a horizontal shift of the recorded horizontal reaction forces at the center column (Fig. 9(b)). Depending on the analysis time, the recorded reaction is either the highest for the lowest live load or vice versa. At this point, no final trend regarding the influence of the live load on the horizontal reaction force at the center column

may be concluded and further investigations on this effect remain a topic of future research. Again, similar tendencies can be observed for the analyzed hybrid RC frames (e.g., Hybrid (6-4) beam, Figs. 9(c) and 9(d)), where the effects seem to be less pronounced.

The investigations on the seismic behavior of RC frames with steel and GFRP reinforcement suggest that hybrid cross-sections can be efficiently applied in hogging moment regions of beams to predetermine the location of potential plastic hinges on RC frames. Moreover, the mechanical properties of GFRP have a beneficial effect on the structural behavior during and after the seismic activity. Depending on the ratio of steel and GFRP reinforcement, the seismic effects on the structure (e.g., column base shear forces) are significantly reduced. Also, the plastic deformations after the earthquake are considerably smaller due to the linear-elastic behavior of the GFRP reinforcement. Both aforementioned effects could enable a reuse of the structure after an earthquake in a more feasible manner.

3.4.5 Future research

The theoretical investigations presented in this paper concentrate on the seismic behavior of one sample RC frame with different plastic hinge reinforcement details (steel-only and steel-GFRP). Obviously, the beneficial effects of GFRP reinforcement in hybrid sections under seismic loads strongly depend on the structural system and the plastic hinge detailing (e.g., connectivity and anchorage of the steel and GFRP reinforcement). Consequently, further investigations are required to quantify the positive influence of hybrid hinges compared to conventional steel-reinforced hinges in a more thorough manner. Moreover, some of the assumptions for the nonlinear finite element simulations need to be confirmed in the future by means of experimental investigations. While the existing flexural tests on hybrid RC beams indicate that basic assumptions like linear distribution of strains remain valid for hybrid sections under static loading (e.g., Refs. [16–19]), experimental proof of these assumptions under cyclic loading is yet to be provided. In addition, the assumption of rigid bond between the reinforcement and the concrete needs to be further investigated in accordance with the results of accompanying experiments and the effect of cyclic loading on the behavior of the GFRP reinforcement would be of interest as its mechanical properties differ in tension and compression. Another aspect for future investigations would be the compatibility between concrete and reinforcement deformations during severe seismic activity.

4 Summary and conclusions

Based on the investigations on the behavior of hybrid

steel-GFRP- RC frames under gravity and seismic loads, the following conclusions can be drawn.

1) In the past, GFRP reinforcement has been applied as an alternative to steel reinforcement in cases where corrosion resistance, electromagnetic neutrality, or cuttability were required. However, due to the low modulus of elasticity, GFRP-RC members usually exhibit large deformations even under service loads, which restricted the wide application of GFRP. A solution to this problem could be the combination of steel and GFRP reinforcement in hybrid cross-sections to exploit the advantages of both materials.

2) Previous investigations indicate that GFRP bars could be efficiently applied in RC structures under seismic loads due to their high deformability and high strength. The investigations presented in this paper support this observation as the combination of steel and GFRP reinforcement at certain locations of RC structures allowed for the creation of plastic hinges at the desired hinge locations. Consequently, hybrid cross-sections could be used in the future as an efficient solution for the predetermination of potential plastic hinges on RC structures.

3) The numerical simulations further indicate that the application of GFRP reinforcement in potential plastic hinges has a positive influence on the overall seismic behavior of RC structures due to the mechanical properties of GFRP. In this context, the horizontal reaction forces of the hybrid sample frames were lower compared to the reference frame. However, a general quantification of this effect is not possible at this point as it strongly depends on each case (e.g., structural system, ratio of steel and GFRP reinforcement, etc.).

4) Finally, the linear-elastic behavior of the GFRP reinforcement resulted in smaller plastic deformations of the hybrid sample frames after the earthquake compared to the conventional steel-only solution. This effect is particularly interesting for the reuse of structures after seismic activity, which could be more feasible for hybrid RC structures than for conventional structures.

Acknowledgements The investigations presented in this paper were supported by Alexander von Humboldt Foundation, Germany, through a Feodor Lynen Research Fellowship for Post-Doctoral Researchers and by a grant from Natural Sciences and Engineering Research Council (NSERC) of Canada. The authors would like to express their sincere gratitude for the support received.

References

1. Kam W Y, Pampanin S. The seismic performance of RC buildings in the 22 February 2011 Christchurch earthquake. *Structural Concrete*, 2011, 12(4): 223–233
2. International Federation for Structural Concrete. FRP Reinforcement in RC Structures. *fib Bulletin* 40. 2007

3. Abdel-Fattah B, Wight J K. Study of moving beam plastic hinging zones for earthquake-resistant design of reinforced concrete buildings. *ACI Structural Journal*, 1987, 84(1): 31–39
4. Al-Haddad M S, Wight J K. Relocating beam plastic hinging zones for earthquake resistant design of reinforced concrete buildings. *ACI Structural Journal*, 1988, 85(2): 123–133
5. Pimanmas A, Chaimahawan P. Shear strength of beam-column joint with enlarged joint area. *Engineering Structures*, 2010, 32(9): 2529–2545
6. Galunic B, Bertero V V, Popov E P. An Approach for Improving Seismic Behavior of Reinforced Concrete Interior Joints. Report UCB/EERC-70/30. 1977
7. Chutarat N, Aboutaha R S. Cyclic response of exterior reinforced concrete beam–column joints reinforced with headed bars—Experimental investigation. *ACI Structural Journal*, 2003, 100(2): 259–264
8. Eom T S, Song J A, Park H G, Kim H S, Lee C N. Cyclic loading test for beam-column connection with prefabricated reinforcing bar details. *ACI Structural Journal*, 2013, 110(3): 403–413
9. Pilakoutas K, Neocleous K, Guadagnini M. Design philosophy issues of fiber reinforced polymer reinforced concrete structures. *Journal of Composites for Construction*, 2002, 6(3): 154–161
10. Sharbatdar M K, Saatcioglu M. Seismic design of FRP reinforced concrete structures. *Asian Journal of Applied Sciences*, 2009, 2(3): 211–222
11. Tavassoli A, Liu J, Sheikh S. Glass fiber-reinforced polymer-reinforced circular columns under simulated seismic loads. *ACI Structural Journal*, 2015, 112(1): 103–114
12. Hasaballa M, El-Salakawy E. Anchorage performance of GFRP headed and bent bars in beam-column joints subjected to seismic loading. *Journal of Composites for Construction*, 2018, 22(6): 04018060
13. Ghomi S K, El-Salakawy E. Seismic behavior of exterior GFRP-RC beam–column connections: Analytical study. *Journal of Composites for Construction*, 2018, 22(4): 04018022
14. Ghomi S K, El-Salakawy E. Effect of joint shear stress on seismic behavior of interior GFRP-RC beam–column joints. *Engineering Structures*, 2019, 191: 583–597
15. Aliasghar-Mamaghani M, Khaloo A. Seismic behavior of concrete moment frame reinforced with GFRP bars. *Composites. Part B, Engineering*, 2019, 163: 324–338
16. Leung H Y, Balendran R V. Flexural behavior of concrete beams internally reinforced with GFRP rods and steel rebars. *Structural Survey*, 2003, 21(4): 146–157
17. Qu W, Zhang X, Huang H. Flexural behavior of concrete beams reinforced with hybrid (GFRP and steel) bars. *Journal of Composites for Construction*, 2009, 13(5): 350–359
18. Safan M. Flexural behavior and design of steel-GFRP reinforced concrete beams. *ACI Structural Journal*, 2013, 110(6): 677–685
19. Maranan G B, Manalo A C, Benmokrane B, Karunasena W, Mendis P, Nguyen T Q. Flexural behavior of geopolymer-concrete beams longitudinally reinforced with GFRP and steel hybrid reinforcements. *Engineering Structures*, 2018, 182: 141–152
20. McKenna F, Fenves G L. Open System for Earthquake Engineering Simulation. 2019 (available at the website of OpenSees)
21. CSA G30.18-09. Carbon Steel Bars for Concrete Reinforcement. Mississauga: Canadian Standard Association, 2014
22. Spacone E, Filippou F C, Taucer F F. Fibre beam–column element for nonlinear analysis of R/C frames. Part I: Formulation. *Earthquake Engineering & Structural Dynamics*, 1996, 25(7): 711–725
23. Mohd Yassin M H. Nonlinear analysis of prestressed concrete structures under monotonic and cycling loads. Dissertation for the Doctoral Degree. Berkeley, CA: University of California, 1994
24. Kent D C, Park R. Flexural members with confined concrete. *Journal of the Structural Division*, 1971, 97(7), 1969–1990
25. Scott B D, Park R, Priestley M J N. Stress-strain behavior of concrete confined by overlapping hoops at low and high strain rates. *ACI Structural Journal*, 1982, 79(1): 13–27
26. Filippou F C, Popov E P, Bertero V V. Effects of Bond Deterioration on Hysteretic Behavior of Reinforced Concrete Joints. Report EERC 83-19. 1983
27. CSA A23.3-14. Design of Concrete Structures. Toronto: Canadian Standard Association, 2015